

Anisotropy Factor Spectra for Weakly Allowed Electronic Transitions in Chiral Ketones

Leon A. Kerber,^[a] Oliver Kreuz,^[b] Tom Ring,^[c] Hendrike Braun,^[c] Robert Berger,^[b] and Daniel M. Reich*^[a]

Quantum chemical calculations of one-photon absorption, electronic circular dichroism and anisotropy factor spectra for the A-band transition of fenchone, camphor and 3-methylcyclopentanone (3MCP) are reported. While the only weakly allowed nature of the transition leads to comparatively large anisotropies, a proper theoretical description of the absorption for such a transition requires to account for non-Condon effects.

We present experimental data for the anisotropy of 3MCP in the liquid phase and show that corresponding Herzberg–Teller corrections are critical to reproduce the main experimental features. The results obtained with our comprehensive theoretical model highlight the importance of the vibrational degree of freedom, paving the way for a deeper understanding of the dynamics in electronic circular dichroism.

1. Introduction

Optically active chiral molecules differ in their absorption of left and right circularly polarized light, this phenomenon is called circular dichroism (CD).^[1] For radiation in the ultraviolet or visible regime the absorption is primarily determined by electronic transitions. In this context the term electronic circular dichroism is used in contrast to, e.g., vibrational circular dichroism in the infrared. While for unpolarized or linearly polarized absorption (ABS) electric dipole transitions constitute the dominant effect, CD is usually very small due to involving both the electric and magnetic transition dipoles. Circular dichroism of an electronic band is primarily characterised via its so-called rotatory strength R , determined by the integral of the difference in absorption over the entire absorption band, and its so-called dipole strength D , the corresponding integral of the unpolarized absorption.^[2] The ratio between CD and ABS yields the so-called anisotropy factor,^[3] also called g -factor or dissymmetry factor.^[2] The anisotropy factor is often considered to be an advantageous observable since it is independent of the sample density and thickness, which can be difficult to characterise in experiments.^[4] Furthermore, the effect of the solvate in liquid-phase experiments seems more readily

apparent in anisotropy factor spectra compared to CD or ABS spectra^[5] and peaks can be assigned with more confidence in high-resolution spectra.^[6]

A particularly favorable class of molecules for the study of circular dichroism are ketones, for which the anisotropy factor of the first singlet electronic excitation band (the A-band) takes on particularly large values in the order of 10^{-1} .^[1] Most notably, the three ketones fenchone, camphor and 3-methylcyclopentanone (3MCP) have been the subject of various theoretical and experimental studies.^[7–21] The origin of the comparatively large anisotropy factors in these systems lies in the only weakly allowed nature of the transition leading to a comparable magnitude of the electric and magnetic transition moments. However, the nature of such a transition requires a particularly careful theoretical treatment.^[22,23] Most importantly, it is necessary to go beyond the Franck–Condon^[24–26] (FC) approximation by including Herzberg–Teller^[27] (HT) contributions.^[1] The combination of Franck–Condon and Herzberg–Teller terms is often abbreviated as FCHT.

One early joint experimental and theoretical study for circular dichroism in ketones was performed in Ref. [7] for fenchone and camphor. However, in their work they only consider vertical transitions, leading to an underestimation of the dipole strength of the A-band. The CD spectrum of 3MCP with the inclusion of HT contributions has first been theoretically examined in Ref. [9] with the latter turning out to be negligible for the A-band. The ABS spectrum was not reported in this work.

Experimentally, both CD and ABS spectra of 3MCP were investigated for absorption in the gas phase^[10–14] as well as the liquid phase.^[13–15] In addition to direct measurements on absorption, circular dichroism also presents itself in ion-yield experiments with several corresponding studies on 3MCP.^[11,12,16–21] In the experiment from Ref. [12] the anisotropy factor spectrum for conventional absorption and ion yield showed similarities, although the anisotropy factor in ion yield was appreciably smaller. This has been attributed to saturation effects due to high power densities in ion yield experiments.^[12,20]

[a] L. A. Kerber, Dr. D. M. Reich

Dahlem Center for Complex Quantum Systems and Fachbereich Physik,
Freie Universität Berlin, D-14195 Berlin, Germany
E-mail: danreich@zedat.fu-berlin.de

[b] O. Kreuz, Prof. Dr. R. Berger

Fachbereich Chemie, Philipps-Universität Marburg, D-35032 Marburg,
Germany

[c] T. Ring, Dr. H. Braun

Institut für Physik, Universität Kassel, D-34132 Kassel, Germany

Supporting information for this article is available on the WWW under
<https://doi.org/10.1002/cphc.202400898>

© 2024 The Author(s). ChemPhysChem published by Wiley-VCH GmbH. This is an open access article under the terms of the Creative Commons Attribution Non-Commercial License, which permits use, distribution and reproduction in any medium, provided the original work is properly cited and is not used for commercial purposes.

However, a comprehensive theoretical treatment of the A-band transition in all three ketones with respect to the HT contributions has hitherto been missing to our knowledge. To amend this, we provide in this work state-of-the-art numerical calculations and compare our results with the experimental literature. We systematically include all Herzberg–Teller contributions and examine their influence on absorption and anisotropy. For 3MCP, we furthermore study the contributions of the two conformational forms. We begin by presenting our calculations for rotatory strengths, dipole strengths, and anisotropy factors of the A-band for all three ketones discussed above. Then, we report results for the vibrational substructure in the electronic spectra. Finally, we also provide an experimental measurement for the anisotropy factor spectrum in 3MCP in solution and compare our theory with this data as well as previous experimental work.

This paper is organised as follows. Section 2 introduces the theoretical model for circular dichroism, unpolarized absorption and the anisotropy factor of the A-band transition. Section 3 presents our numerical results, comparing with the literature as well as our own measurements of the anisotropy in 3MCP in the liquid phase. Finally, section 4 provides our conclusions and research directions for future work.

2. Methods

The A-band corresponds to a transition from the electronic ground state S_0 , referred to by index i in the following, to the first electronically excited singlet state S_1 , referred to by index f . We write $|i\mathbf{v}_i\rangle$ and $|f\mathbf{v}_f\rangle$ for the vibronic levels with \mathbf{v}_i and \mathbf{v}_f being the vibrational levels in the electronic states i and f , respectively. Similarly to Ref. [9], we neglect the rotational degrees of freedom in our modeling of the molecular states. We employ SI units throughout this section unless noted otherwise. The electronic part of the electric dipole moment operator is then given by:

$$\hat{\boldsymbol{\mu}} = - \sum_{j=1}^{n_e} e \hat{\mathbf{q}}_j, \quad (1)$$

where n_e denotes the total number of electrons, e is the elementary charge and $\hat{\mathbf{q}}_j$ denotes the position operator of the j th electron. The spin-independent electronic part of the magnetic dipole moment operator is given by:

$$\hat{\mathbf{m}} = - \sum_{j=1}^{n_e} \frac{e}{2m_e} (\hat{\mathbf{q}}_j \times \hat{\mathbf{p}}_j), \quad (2)$$

where m_e is the electron mass and $\hat{\mathbf{p}}_j$ denotes the linear momentum operator of the j th electron. Within the Born–Oppenheimer approximation,^[28] the matrix elements of these operators between vibronic levels can be evaluated first in the electronic degrees of freedom. The electronic states depend parametrically on the nuclear coordinates, but are orthonormal at

each nuclear arrangement. Consequently, nuclear parts that depend on positions and momenta of the nuclei and contribute besides the electronic parts given in Eqs. (1) and (2) to the total dipole operators cannot contribute in this approximation, when the vibronic levels of interest are assigned to different electronic levels. Moreover, since spin-orbit coupling is expected to be small for the ketones we study in our work and since transitions between electronic singlet states are considered, the electron spin contribution to the magnetic transition dipole moments is dropped for the present study.^[29] After integrating out the electronic degrees of freedom, electronic transition matrix elements $\hat{\boldsymbol{\mu}}_{fi}$ and $\hat{\mathbf{m}}_{fi}$ of the dipole operators remain that depend parametrically on the nuclear coordinates and for which then matrix elements in the vibrational manifold have to be computed. For this purpose, we now expand the electronic transition matrix elements of $\hat{\boldsymbol{\mu}}$ with respect to the electronic ground state's normal coordinates $\mathbf{Q} = \{Q_r\}$ defined relative to the equilibrium position $\mathbf{Q} = \mathbf{0}$. For the electronic part of the electric transition dipole moment to first order this yields:

$$\boldsymbol{\mu}_{fi}(\mathbf{Q}) \approx \boldsymbol{\mu}_{fi}(\mathbf{0}) + \sum_r \frac{\partial \boldsymbol{\mu}_{fi}}{\partial Q_r}(\mathbf{0}) Q_r \quad (3)$$

with the corresponding expression for the magnetic transition dipole moment following analogously. We use the harmonic approximation for the potential energy surfaces of the two electronic states, and therefore neglect terms that would formally arise in a series expansion in the same order as the electric and magnetic anharmonicities. As a consequence, all vibrational levels for an electronic state a are considered as tensor products of harmonic oscillator eigenstates $|v_{r,a}\rangle$, where $r \in \{1, 2, \dots, 3N-6\}$ indicates the different vibrational modes. This means that $|v_a\rangle = |v_{1,a}\rangle \otimes |v_{2,a}\rangle \otimes \dots \otimes |v_{3N-6,a}\rangle$ with N the number of atoms in the molecule. Finally, we consider the system at room temperature, that is $T = 300$ K. Correspondingly, all results from our calculations are averaged over the set of initial vibrational states $|v_i\rangle$ weighted by their respective Boltzmann probabilities p_{v_i} .

The vibronic matrix elements are then given by:

$$\boldsymbol{\mu}_{fv_i,iv_i} \approx \boldsymbol{\mu}_{fi}(\mathbf{0}) \langle \mathbf{v}_f | \mathbf{v}_i \rangle + \sum_r \frac{\partial \boldsymbol{\mu}_{fi}}{\partial Q_r}(\mathbf{0}) \langle \mathbf{v}_f | \hat{Q}_r | \mathbf{v}_i \rangle, \quad (4)$$

and similarly for \mathbf{m}_{fv_i,iv_i} . The first term contains the Franck–Condon overlap integral $\langle \mathbf{v}_f | \mathbf{v}_i \rangle$ whereas the second term involves the Herzberg–Teller overlap integrals.^[27] In the following we refer to the first summand of Eq. (4) as Franck–Condon term and to the second summand as Herzberg–Teller term.

The A-band, i.e. the $S_0 \rightarrow S_1$ transition, corresponds approximately to an $n \rightarrow \pi^*$ transition in the carbonyl group of the ketones. In a simplified one-particle picture, this is associated with an electron changing from a nonbinding orbital confined to the O atom to an antibonding π^* orbital spread over the C and O atoms of the carbonyl group. In the Franck–Condon approximation and when additionally assuming C_{2v} point group symmetry of a ketone that coincides with the local C_{2v} symmetry of the carbonyl group, this transition is electric

dipole-forbidden and magnetic dipole-allowed.^[30,31] When overall point group symmetry is lowered, for instance to chiral C_2 or, as in the present cases, to C_1 , the selection rule for the electric transition dipole term becomes lifted. Under these circumstances, $\mu_{fi}(\mathbf{0})$ and thus the Franck–Condon term is very small such that the Herzberg–Teller term becomes important. Conversely, for the magnetic transition dipole moment, the Franck–Condon term is expected to provide a good approximation since the transition is magnetic-dipole allowed.^[1,22] Nevertheless we include both contributions to the magnetic transition dipole moment in our calculations for consistency.

Our main goal is to determine anisotropy factors, defined as the ratio of circular dichroism to unpolarized absorption.^[1] These quantities can both be investigated in a frequency-dependent manner, highlighting the vibronic structure of the transition in question, or as “band values” obtained via integration over the entire absorption band. From a theoretical point of view, the band values are accessible with much less effort, as no knowledge about the excited state vibrational structure is required.^[1] On the other hand, the full spectra reveal much more detailed information on the role of the vibrational degree of freedom and serve as a more sensitive benchmark when comparing with experiments.

The CD spectrum is commonly expressed as the difference between the molar absorption coefficients of left and right circularly polarized light as a function of the frequency of incident electromagnetic radiation,^[1,32] i.e., $\Delta\varepsilon(\omega) = \varepsilon_L(\omega) - \varepsilon_R(\omega)$. For a randomly oriented ensemble, considering only electric and magnetic dipole interactions between the molecules and the radiation, resonant excitation with left-circularly and right-circularly polarized light leads in first order perturbation theory to an absorption difference proportional to the imaginary part of the scalar product of the corresponding electric and magnetic transition dipole moments.^[32,33] This scalar product constitutes the so-called rotatory strength of the transition.^[34] Therefore, there is a rotatory strength connected to each vibronic transition of the CD spectrum,

$$R_{f\nu_i\nu_i} = \text{Im}\{\boldsymbol{\mu}_{i\nu_i f\nu_i} \cdot \mathbf{m}_{f\nu_i i\nu_i}\}. \quad (5)$$

The connection between the CD spectrum and these quantities is given by:^[32,35]

$$\begin{aligned} \Delta\varepsilon(\omega) &= \frac{16\pi^2 N_A \omega}{3(4\pi\varepsilon_0)\hbar c^2 \ln 10} \sum_{\nu_i, \nu_i} p_{\nu_i} \rho(\omega, \omega_{f\nu_i i\nu_i}) R_{f\nu_i i\nu_i} \\ \Delta\varepsilon(\omega)/(\text{cm}^2 \text{mmol}^{-1}) &= 20.529 \times (\omega/(E_h \hbar^{-1})) \\ &\quad \sum_{\nu_i, \nu_i} p_{\nu_i} (\rho(\omega, \omega_{f\nu_i i\nu_i})/(\hbar E_h^{-1})) (R_{f\nu_i i\nu_i}/(e^2 a_0 \hbar^2 m_e^{-1})), \end{aligned} \quad (6)$$

where N_A is the Avogadro number and $\rho(\omega, \omega_{f\nu_i i\nu_i})$ is a normalized line shape function, introducing a line width to each transition $|f\nu_i\rangle \leftarrow |i\nu_i\rangle$ with transition frequency $\omega_{f\nu_i i\nu_i}$. The spectrum is averaged over initial vibrational states ν_i weighted by their respective Boltzmann probabilities p_{ν_i} at $T=300$ K. Since the A-band of the three ketones in our work does not overlap with any other absorption bands it is not necessary to

sum over other electronic states in Eq. (6). Note that we adjusted the prefactor in Eq. (6) compared to Ref. [9] to match our definition of the rotatory strength.

The ABS spectrum is defined as the mean absorption of left and right circularly polarized light, $\varepsilon(\omega) = \frac{1}{2}(\varepsilon_L(\omega) + \varepsilon_R(\omega))$ or, equivalently, of unpolarized light. Similar to how the CD spectrum is connected to the rotatory strength, the ABS spectrum is connected to the so-called dipole strength of the involved vibronic transitions, given by the sum of the absolute value squares of electric and magnetic transition dipole moments,

$$D_{f\nu_i i\nu_i} = |\boldsymbol{\mu}_{f\nu_i i\nu_i}|^2 + \left(\frac{|\mathbf{m}_{f\nu_i i\nu_i}|}{c}\right)^2. \quad (7)$$

The connection between these quantities is given by:^[32]

$$\begin{aligned} \varepsilon(\omega) &= \frac{4\pi^2 N_A \omega}{3(4\pi\varepsilon_0)\hbar c \ln 10} \sum_{\nu_i, \nu_i} p_{\nu_i} \rho(\omega, \omega_{f\nu_i i\nu_i}) D_{f\nu_i i\nu_i} \\ \varepsilon(\omega)/(\text{cm}^2 \text{mmol}^{-1}) &= 703.301 \times (\omega/(E_h \hbar^{-1})) \\ &\quad \sum_{\nu_i, \nu_i} p_{\nu_i} (\rho(\omega, \omega_{f\nu_i i\nu_i})/(\hbar E_h^{-1})) (D_{f\nu_i i\nu_i}/(e^2 a_0^2)). \end{aligned} \quad (8)$$

The anisotropy factor spectrum is given as the ratio of CD and ABS, i.e.,

$$g(\omega) = \frac{\Delta\varepsilon(\omega)}{\varepsilon(\omega)}. \quad (9)$$

Note that if only the Franck–Condon terms are considered and the line-shape functions for CD and ABS are identical,^[32] the anisotropy factor becomes frequency-independent for a given absorption band, since the sums involving products of Franck–Condon factors, Boltzmann probabilities and line shape function appear both in the numerator and denominator of Eq. (9) and thus cancel. However, the more complicated structure of the anisotropy seen in experiments^[36] suggests the necessity to include Herzberg–Teller effects. As such, to perform adequate calculations of the CD and ABS spectra, the vibrational fine structure of the excited state needs to be taken into account.

For determining the rotatory strength of the *entire absorption band*, in contrast, the vibrational fine structure of the excited state does not play a role. This can be understood by employing the resolution of the identity via the final state vibrational manifold, $\sum_{\nu_f} |\nu_f\rangle \langle \nu_f| = \mathbb{1}$, leading to the following expression,^[9]

$$\begin{aligned} R_{fi} &= \frac{3(4\pi\varepsilon_0)\hbar c^2 \ln 10}{16\pi^2 N_A} \int_{\text{A-band}} \frac{\Delta\varepsilon}{\omega} d\omega \\ &= \sum_{\nu_i, \nu_i} p_{\nu_i} \text{Im}\{\boldsymbol{\mu}_{i\nu_i f\nu_i} \cdot \mathbf{m}_{f\nu_i i\nu_i}\} \\ &\approx \text{Im}\{\boldsymbol{\mu}_{fi}(\mathbf{0}) \cdot \mathbf{m}_{fi}(\mathbf{0}) \\ &\quad + \sum_{r, \nu_f} p_{\nu_f} \frac{\partial \boldsymbol{\mu}_{fi}}{\partial Q_r}(\mathbf{0}) \cdot \frac{\partial \mathbf{m}_{fi}}{\partial Q_r}(\mathbf{0}) \langle \nu_f | \hat{Q}_r^2 | \nu_i \rangle\}. \end{aligned} \quad (10)$$

Here and in the following, we included FC and linear HT terms for both the electric and magnetic transition dipole moments. We considered the harmonic approximation in the initial states, which implies that $\langle \mathbf{v}_i | \hat{Q}_r | \mathbf{v}_i \rangle = 0$ and $\langle \mathbf{v}_i | \hat{Q}_r^2 | \mathbf{v}_i \rangle = (n_{r,i} + \frac{1}{2}) \frac{\hbar}{\omega_{r,i}}$, with $n_{r,i}$ and $\omega_{r,i}$ denoting the excitation number and angular frequency of the r -th mode of the vibrational configuration \mathbf{v}_i , respectively. Eq. (10) shows that the integrated rotatory strength consists of the FC term, depending only on the equilibrium structure, and a HT correction. This correction depends on the variances of the normal coordinates in the initial states and the product of the first derivatives of the transition dipole moments. Note that due to the magnetic-dipole allowed nature of the transition, the HT correction is usually assumed to be small and the FC rotatory strength is expected to represent an adequate approximation. Analogously to the band-integrated rotatory strength, the band-integrated dipole strength is unaffected by the final-state vibrational structure yet depends on the variances of the normal coordinates in the initial states,

$$D_{fi} = \frac{3(4\pi\epsilon_0)\hbar c \ln 10}{4\pi^2 N_A} \int_{\text{A-band}} \frac{\epsilon}{\omega} d\omega$$

$$\approx |\boldsymbol{\mu}_{fi}(\mathbf{0})|^2 + \sum_{r,\mathbf{v}_i} \rho_{\mathbf{v}_i} \left| \frac{\partial \boldsymbol{\mu}_{fi}}{\partial Q_r}(\mathbf{0}) \right|^2 \langle \mathbf{v}_i | \hat{Q}_r^2 | \mathbf{v}_i \rangle$$

$$+ \frac{1}{c^2} \left(|\mathbf{m}_{fi}(\mathbf{0})|^2 + \sum_{r,\mathbf{v}_i} \rho_{\mathbf{v}_i} \left| \frac{\partial \mathbf{m}_{fi}}{\partial Q_r}(\mathbf{0}) \right|^2 \langle \mathbf{v}_i | \hat{Q}_r^2 | \mathbf{v}_i \rangle \right). \quad (11)$$

However, in contrast to the rotatory strength, even if the magnetic HT contribution is negligible, the electric HT contribution remains potentially important for the band-integrated dipole strength.

Using Eqs. (10) and (11) we can assign an anisotropy factor to the entire electronic band via,^[1]

$$g = \frac{4R_{fi}/c}{D_{fi}}. \quad (12)$$

As mentioned before, in the FC case, the anisotropy factor spectrum of Eq. (9) takes on a constant value over the band. This value then coincides with the band value of Eq. (12), that is $g(\omega) = g$, in this case. However, in general the anisotropy factor spectrum is not represented by a constant and no such connection can be made.^[1,32] Furthermore, some chiral molecules exist in different conformers at room temperature. For the molecules examined in this work, this is the case for 3MCP. For a mixture of conformers c contained in proportions of p_c , spectra and integrated band values will be superimposed accordingly, e.g. Eq. (9) becomes in that case,

$$g(\omega) = \frac{\sum_c p_c \Delta \epsilon_c(\omega)}{\sum_c p_c \epsilon_c(\omega)}. \quad (13)$$

Note that Eq. (13) tells us that in the case of a conformational mixture the anisotropy factor can generally be frequency-dependent even in the Franck–Condon case.

To theoretically predict the integrated quantities of Eqs. (10) to (12), we first determine the equilibrium structure of the electronic ground state S_0 and its corresponding vibrational structure within the harmonic approximation. Then, the transition dipole moments and derivatives of the electric transition dipole moment are computed. Determination of the vibrationally resolved spectra represented by Eqs. (6), (8) and (9) requires in our approximation also knowledge of the equilibrium structure and harmonic force field of the energetically lowest electronic singlet state S_1 . In the time-independent framework, individual Franck–Condon integrals and Herzberg–Teller terms are computed. In the complementary time-dependent framework the spectral shape is calculated by exploiting the link between the time-correlation function (TCF) and the coherent-states based generating function (GF) for the FCHT integrals.^[39,40] The possibility to compute CD spectra employing the TCF approach was first outlined by Abbate et al. in Ref. [41] and explicitly applied by Seibt and Engel in Ref. [42]. An extension to vibrationally resolved spectra including linear terms of both the magnetic and electric dipole derivatives was given in Ref. [43]. For ketones, determination of vibrationally resolved spectra is complicated by the fact that the S_1 state of carbonyl compounds typically features two viable minima on its potential energy surface.^[9] This is due to pyramidalization of the carbonylic C atom, which can take place in two different directions. To account for this, we determined the structure of the transition state between both minima, which corresponds to a nearly planar arrangement around the carbonylic C atom. This stationary point on the S_1 potential energy surface results in an imaginary vibrational frequency for the mode responsible for pyramidalization. One could attempt to describe the resulting pyramidalization motion within an effective one-dimensional anharmonic model to capture the corresponding anharmonic progressions in this mode. Another possibility is to choose instead a rather crude and pragmatic model, in which the imaginary vibrational frequency is either replaced by the real frequency of the mode of the S_0 state with the highest overlap or by its absolute value. In this work we chose the latter approach. Moreover, to determine the 0–0 transition energy we used the adiabatic excitation energy to the transition structure in S_1 and corrected for the difference in the zero-point vibrational energies with neglect of the imaginary harmonic frequency. The equilibrium structures and harmonic vibrational force fields of the compounds were determined using the Turbomole software package^[44] (Version 7.6). Molecular structures were energy-minimized using density functional theory (DFT) at the B3-LYP/def2-TZVP level of theory^[45–48] with the resolution of the identity method for the Coulomb part (RI-J)^[49] enabled on the m4 numerical integration grid with D3 dispersion correction^[50] with damping (BJ).^[51] More details and results of the quantum chemical calculations are given in the supplementary information.^[52] The vibrational frequencies and normal modes were obtained in the harmonic approximation of the respective potential energy surfaces at their respective structures. Calculation of Franck–Condon and Herzberg–Teller integrals as well as of the spectral shapes via the time-dependent framework were performed with a modified version

of the hotFCHT code.^[39,53–55] The Boltzmann averages for the band values were also calculated analytically^[43] with the modified hotFCHT code.

3. Results

Figure 1 shows the results of the integrated band values according to Eqs. (10) to (12) for the three ketones (1R,4S)-(–)-fenchone, (1S,4S)-(–)-camphor and (R)-(+)-3-methylcyclopentanone.

To compare our calculations with theoretical and experimental data from the literature, we first computed all quantities by only considering the Franck–Condon terms (abbreviated as “FC” in the figure). Then, we recalculated all quantities including both the Franck–Condon and Herzberg–Teller terms (abbreviated as “FCHT” in the figure) for the dipole moments. We compare our calculations to the experimental and theoretical results of Ref. [7]. Based on the reported band-integrated rotatory strengths R and oscillator strengths f as well as band peak positions ω_0 , we determined the anisotropy factors according to^[11] $D \approx \frac{3\hbar e^2}{2m_e \omega_0} f$ and Eq. (12). When referencing the literature for these quantities, we always consider the derived values.

We observe that the experimental anisotropy factor values differ significantly from the numerical FC results. Specifically, neglecting the HT contribution overestimates the absolute value of the anisotropy factor by an order of magnitude for

fenchone and a factor of two for camphor. By including these terms the agreement with the experimental values is vastly improved. We attribute this improvement to the large effect of the inclusion of the electric dipole HT terms on the dipole strengths since the magnetic dipole HT term only contributes with less than 0.1% of the total value. This is in accordance with the expected behaviour resulting from the magnetic-dipole allowed nature of the transition. Conversely, the HT correction to the rotatory strengths, which is due to the product of electric and magnetic HT terms, is small yet significant. The discrepancy between our FC calculations and the theoretical results from Ref. [7] for the rotatory strength is due to differences in the numerical approach.

The ketone 3MCP exists in five conformational forms at room temperature with the equatorial and axial conformers constituting the main components. The ratio between these two conformers has been determined using three different approaches in Ref. [37] yielding proportions of 87:13, 78:22 and 70:30 equatorial:axial 3MCP. However, we do not consider the 70:30 ratio in the following, due to the large uncertainty associated with this particular result. Instead we show results both for a ratio of 87:13, which was obtained via temperature-dependent vibrational absorption intensities (dotted pattern in Figure 1), and for a ratio of 78:22, which was obtained from comparison of theoretically and experimentally determined specific rotations (striped pattern in Figure 1). The first ratio coincides with REMPI investigations in the gas phase^[56] and the latter ratio coincides with a study of conformational proportions in a variety of solvents.^[38]

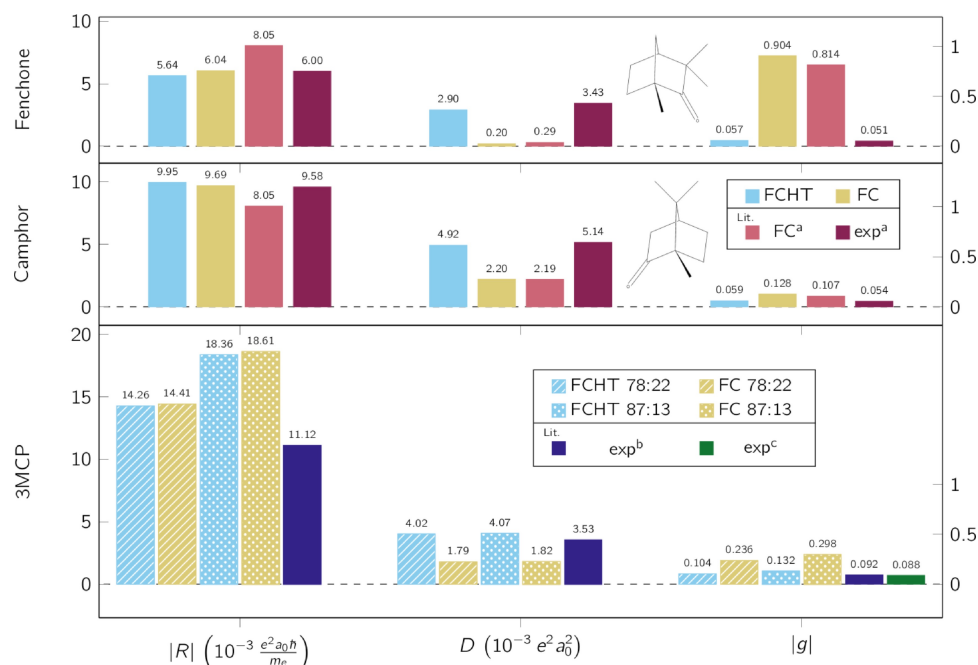


Figure 1. Comparison of theoretical and experimental results for absolute value of rotatory strength, dipole strength (left axis) and absolute value of anisotropy factor (right axis) for fenchone, camphor and 3MCP at room temperature. Theoretical results obtained by including the Franck–Condon and Herzberg–Teller terms for the transition dipole moments are denoted by FCHT, those obtained only including the Franck–Condon term by FC. The results of the present work are compared to various theoretical^{[7]a} and experimental^{[7]a,[10]b,[15]c} values from the literature. The literature values for dipole strengths and anisotropy factors and the rotatory strength for 3MCP refer to derived quantities, see main text for further details. For 3MCP, our results are shown for two different mixtures of the equatorial and axial conformers, 87:13 and 78:22.^[37,38]

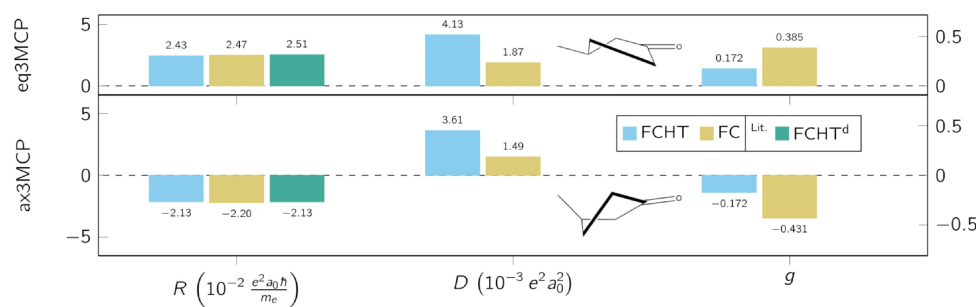


Figure 2. Theoretical results of rotatory strength, dipole strength (left axis) and anisotropy factor (right axis) for equatorial and axial 3MCP conformers at room temperature. Theoretical results obtained by including the Franck–Condon and Herzberg–Teller terms for the transition dipole moments are denoted by FCHT, those obtained only including the Franck–Condon term by FC. The results of the rotatory strengths are compared to a similar theoretical study.^{[9]d}

We performed our calculations by first determining the relevant quantities of the equatorial and axial conformers, respectively, and then calculating, e.g., the anisotropy according to Eq. (13) with the corresponding proportions of the conformers.

For 3MCP we extracted experimental band values from Refs. [10,15] by digitizing the spectra and calculating the corresponding integrals for the band values. These experiments encompass both gas-phase measurements^[10] and measurements in solution with n-heptane.^[15] The values for the band anisotropy factor agree between both experiments. Comparison with the spectra was complicated by the low resolution in Ref. [10]. Additionally, in Ref. [15] the spectra were only recorded to about 270 nm. Nevertheless, these spectra are suitable as a qualitative benchmark for our calculations. Figure 2 shows the results for the individual conformers of 3MCP.

Since both conformers have similar dipole strengths, but opposite sign in their rotatory strength, the ratio of the mixture between the conformers mainly affects the rotatory strength and the anisotropy. The inclusion of the HT terms doubles the dipole strengths for both individual conformers and halves the magnitude of the anisotropy factors accordingly. Our results for the two conformers agree with a similar theoretical estimate of the rotatory strength from the literature.^[9] Similarly to Ref. [9], the impact of the HT correction on the rotatory strength we observe is much weaker than in our calculations for fenchone and camphor.

Our numerically calculated anisotropy factor spectra for 3MCP are shown in Figure 3. Similarly to the band-integrated data in Figures 1 and 2, we show our results for the anisotropy factor spectra once obtained with (FCHT, solid blue line) and without (FC, solid yellow line) the inclusion of HT terms. Here and in the following we only show our theoretical results inside the A-band, omitting the data points where the A-band absorption approaches zero as this regime is not well-captured by our model. The spectra were generated assuming a conformational mixture of 78:22 equatorial to axial 3MCP.^[37,38] For the line shape function, we employed a Lorentzian profile of 0.03 eV full width half maximum, in view of obtaining good agreement with the experimental spectra. The magnetic contributions to the band-integrated dipole strength lie well below 1% for all three ketones in our study. In contrast to the

CD spectra, there is no possibility of potentially large individual negative and positive contributions to cancel such that we were able to neglect these contributions to the ABS spectra in Eq. (7) in our calculations.

We compare our calculated anisotropy factor spectra with a conventional measurement of differential absorption and absorption of 3MCP in the gas phase.^[11] The shown anisotropy factor spectrum was generated by digitizing the corresponding spectra and plotting their ratio. We furthermore compare the spectra with our own experimentally obtained liquid-phase spectrum of 3MCP. The respective absorption studies were solely performed on the (R)-enantiomer (Sigma Aldrich, constitutional purity 99.8%). The substance was used without further purification and dissolved in the non-polar solvent n-hexane. We employed a circular dichroism spectropolarimeter (J-815, Jasco) to measure the relative absorbance of a solution of 65 mL 3-methylcyclopentanone in 935 mL n-hexane. An average of six consecutive measurements with step size and bandwidth of 0.5 nm was considered. The background by the solvent was determined separately and subtracted. A UV/Visible spectrophotometer (Cary 100, Varian) with simultaneous acquisition of background and sample absorbance was used to evaluate the absolute absorption. The step size was 0.5 nm, and the bandwidth was increased to 1 nm. Here, 20 mL 3MCP were dissolved in 10 mL n-hexane for good signal-to-noise-ratio. In the region close to 200 nm, the cutoffs of the quartz cuvettes containing the samples and n-hexane are reached, i.e., their absorption increases already for larger wavelengths. In addition, the CD data from the first measurement becomes noisy in this wavelength region. The next strong absorption band with pronounced CD is located in the wavelength region from 200 nm to 185 nm, according to Ref. [10], but cannot be observed under the present measurement conditions. Compared to the gas phase,^[11] the liquid-phase measurement using the non-polar solvent n-hexane only shows a soft hypsochromic shift (~0.5 nm).

Our FCHT calculations reproduce the most important features of the experimental spectra of 3MCP very well. Specifically, the sign and overall magnitude of the anisotropy factor is well-reproduced and the position of the main peaks at around 300 nm, 310 nm and 320 nm matches. Moreover, the peak heights increase from smaller to larger wavelengths with

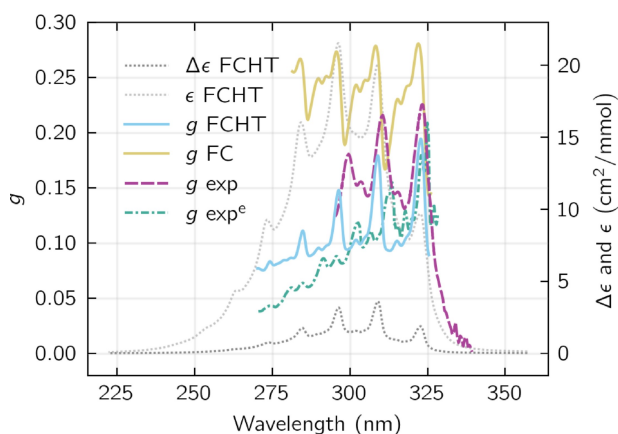


Figure 3. Theoretical (FC and FCHT) anisotropy factor spectra (g , left axis) of 3MCP at room temperature, assuming a conformational mixture of 78:22 equatorial to axial 3MCP in comparison with our experimental liquid-phase spectrum and the conventional (differential) absorption measurements of Ref. [11]e. The FCHT anisotropy factor spectrum has been generated from the shown CD ($\Delta\epsilon$) and ABS (ϵ) spectra (right axis). A Lorentzian line shape with a FWHM of 0.03 eV has been applied for CD and ABS spectra.

several smaller peaks interspersed. We thus expect our calculations to capture the main influence of the vibronic structure of 3MCP on the anisotropy factor. Our anisotropy factor spectrum for the FC case deviates from a simple constant value due to the mixture of conformers. Even without HT corrections, the positions of the peaks of the experimental spectra are well reproduced, however, the magnitudes are not.

Figure 4 unravels the source of the differences between FC and FCHT anisotropy factor spectra. CD and ABS spectra are displayed for both the axial and equatorial conformers. The spectral position of the A-band for the axial conformer is found to be at 0.017 eV below the spectral position for the equatorial conformer. This coincides with experimental findings for the energy shift of the B-band.^[56] For the spectra of equatorial 3MCP as well as the conformational mixture, the main peaks are approximately located at 323 nm, 309 nm, 296 nm, 284 nm, and 273 nm. The peak separation is about 0.17 eV, corresponding to the energy of the C–O stretching mode. A detailed discussion of the vibrational structure has been given elsewhere.^[9,11] In agreement with other theoretical studies,^[9] our results show that Herzberg–Teller contributions do not affect the CD spectrum in the case of 3MCP. A possible explanation was given in the literature.^[9] Therein, a lack of energetically close large intensity transitions was considered to prevent a large intensity borrowing effect. However, this reasoning has been questioned before^[57] and, in fact, does not appear to provide an adequate explanation to our results. Specifically, as evidenced by the bottom panels of Figure 4 the Herzberg–Teller effect significantly alters the ABS spectrum.

For fenchone and camphor, we chose a Lorentzian profile of 0.04 eV full width half maximum for the line shape function. This choice was made in view of obtaining good agreement with the experimental spectra of Ref. [7]. The inclusion of the Herzberg–Teller terms leads to some deformation of the CD spectrum when compared to the Franck–Condon results shown

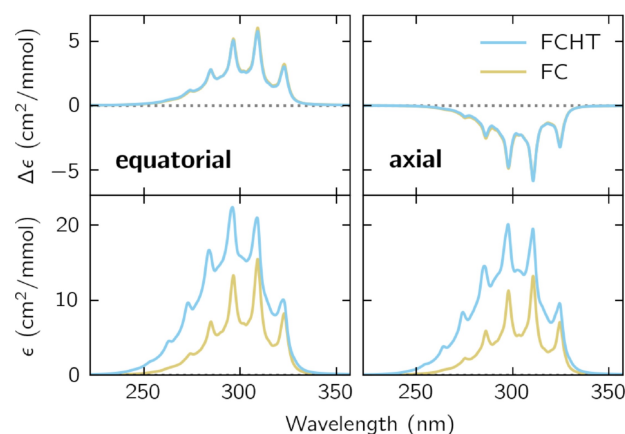


Figure 4. Theoretical CD (upper plots) and ABS (lower plots) spectra of equatorial and axial 3MCP at room temperature comparing the results for FC and FCHT calculations. A Lorentzian line shape with a FWHM of 0.03 eV has been employed.

in Figure 5. However, on a qualitative level the curves do not differ appreciably with a significant impact of the Herzberg–Teller terms only visible for the ABS spectra. Our theoretical FCHT results show a good agreement with the experimental CD data and a strong improvement towards the experimental ABS spectra. Notably, the intensities of the FC-level ABS spectra are considerably too low whereas the FCHT anisotropy factor spectra in Figures 6 and 7 correctly reproduce the overall magnitude of the anisotropy factor. In the case of camphor, qualitative features like the rise until around 300 nm and the peak at around 315 nm are shared with the experimental spectrum. The Franck–Condon case in Figure 6 shows the expected constant anisotropy factor spectrum at the band value, cf. Figure 1. For fenchone, the theoretical ABS spectrum still falls somewhat short of the experimentally observed magnitudes and appears slightly shifted in energy compared to the experimental data. Even though the general trend of the anisotropy factor matches between theory and experiment the quantitative agreement is somewhat weaker than for 3MCP and camphor.

From the theoretical side, we attribute the remaining discrepancies between our calculations and the experimental data to several potential causes. First, there is an inherent limited accuracy in our quantum chemical calculations. This concerns especially equilibrium structures, transition dipole moments and their derivatives with respect to displacements along the normal modes, as well as transition energies. Second, the conformer ratio of 3MCP is particularly relevant to the CD spectra and the rotatory strength but unfortunately not precisely known. Third, the quantum chemical calculations performed in this work do not consider any interactions between the molecules or between the molecules and a solvent, which limits our ability to reproduce experimental results recorded in the liquid phase. This is particularly relevant for 3MCP since both conformers can be affected differently by the solvent. Fourth, the Lorentz profiles constitute a simplification of the actual broadening profiles stemming in the main part from thermal broadening in the rotational degree of

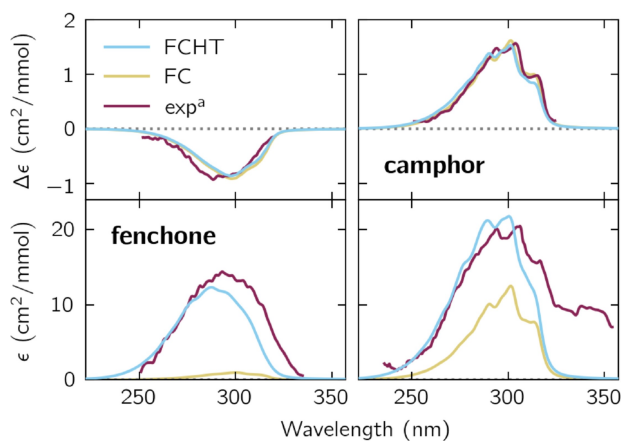


Figure 5. Theoretical CD (upper plots) and ABS (lower plots) spectra of fenchone and camphor at room temperature comparing the results for FC and FCHT calculations with experimental spectra.^{[7]a} A Lorentzian line shape with a FWHM of 0.04 eV has been employed for the theoretical spectra.

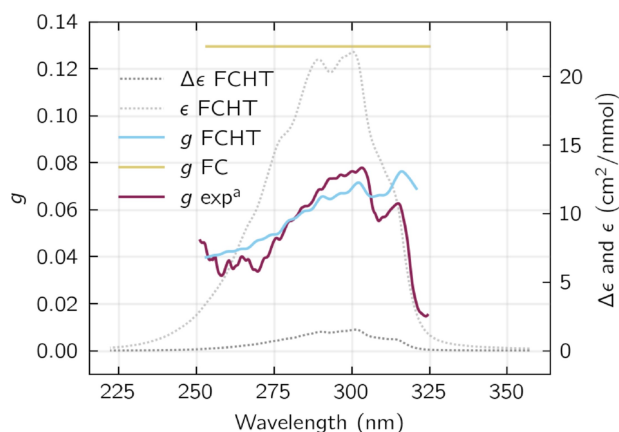


Figure 6. Theoretical (FC and FCHT) and experimental^{[7]a} anisotropy factor spectra (g , left axis) of camphor at room temperature. The FCHT anisotropy factor spectrum has been generated from the shown CD ($\Delta\epsilon$) and ABS (ϵ) spectra (right axis). A Lorentzian line shape with a FWHM of 0.04 eV has been employed for CD and ABS spectra. Note that we flipped the sign for our theoretical CD and anisotropy factor spectra to match the enantiomer examined in the experiment.

freedom and bandwidth of the incident radiation. Lastly, the approximation of the potential energy surfaces as harmonic potentials is a strong simplification.

4. Conclusions

We have calculated the absorption and anisotropy factor spectra for the A-band transition in the three ketones (1R,4S)-(-)-fenchone, (1S,4S)-(-)-camphor and (R)-(+)-3-methylcyclopentanone. To this end we employed quantum chemistry calculations at the DFT level in the harmonic approximation to determine vibrational frequencies and normal modes in the corresponding electronic states. By including the Herzberg–Teller contribution in the vibronic matrix elements for both transition dipole moments we obtained both frequency-

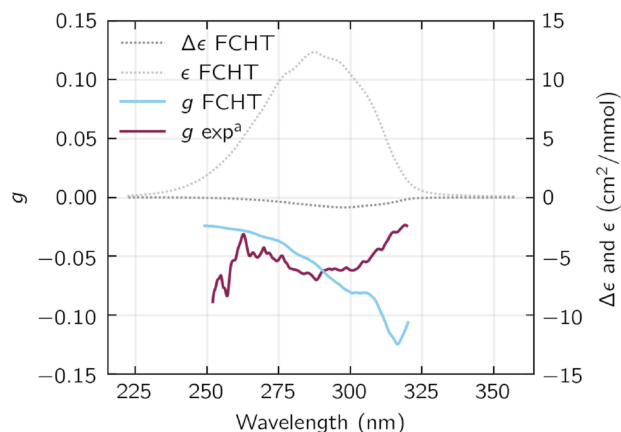


Figure 7. Theoretical (FCHT) and experimental^{[7]a} anisotropy factor spectra (g , left axis) of fenchone at room temperature. The FCHT anisotropy factor spectrum has been generated from the shown CD ($\Delta\epsilon$) and ABS (ϵ) spectra (right axis). A Lorentzian line shape with a FWHM of 0.04 eV has been employed for CD and ABS spectra. The FC anisotropy factor is given by a flat line at the band value, cf. Figure 1. It is not shown in the figure due to its large magnitude compared to the FCHT, respectively experimental, values.

resolved absorption and anisotropy factor spectra as well as the corresponding band-integrated results. Even though their impact on the difference in absorption between the enantiomers is small, we found that the Herzberg–Teller contributions are crucial to understand the structure of the absorption spectra and therefore also the anisotropy. Furthermore, when only considering the Franck–Condon contributions the band-integrated value of the anisotropy can differ by up to an order of magnitude as evidenced by fenchone. This highlights the critical importance of the Herzberg–Teller effect when investigating circular dichroism in the approximately electric dipole-forbidden transitions for which particular large dichroic signatures can be observed in absorption.

Our calculations show good agreement with experimental data for all three ketones. Particularly for 3MCP we are able to reproduce many central features of the experimentally reported anisotropy spectra. Although our agreement for fenchone is somewhat weaker we are still able to reproduce the general magnitude and most important qualitative features.

Our results pave the way for an improved modeling of circular dichroism experiments in ketones. This is of particular importance for understanding the role of the vibrational degree of freedom on the anisotropy when using shaped, e.g. chirped, laser pulses. The interplay between the chirp and the vibrational structure can be an important resource for coherent control as has been evidenced for example in the photoassociation of Mg_2 dimers.^[58,59] Moreover, the improved modeling of the vibronic transitions will be an important asset to lift studies on optimal control of circular dichroism from few-level systems closer to physical reality.^[60] Finally, to understand the difference in anisotropy between absorption and ion yield we expect that further theoretical investigations in the role of higher-lying electronic excited states are required which will be subject to future work.

Acknowledgements

We thank the AG Biophysik by Prof. Kleinschmidt at Universität Kassel for their support in recording the anisotropy factor spectrum for 3MCP. Computer time provided by the Center for Scientific Computing (CSC) Frankfurt is gratefully acknowledged. This work is funded by the Deutsche Forschungsgemeinschaft (DFG, German Research Foundation) – Projekt-nummer 328961117 – SFB ELCH 1319. Open Access funding enabled and organized by Projekt DEAL.

Conflict of Interests

The authors declare no conflict of interest.

Data Availability Statement

The data that support the findings of this study are available in the supplementary material of this article.

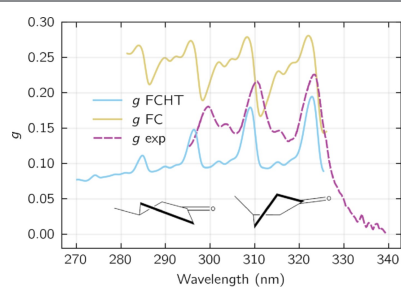
Keywords: chirality · circular dichroism · ketones · absorption · quantum chemistry

- [1] K. Nakanishi, N. Berova, R. W. Woody, *Circular Dichroism: Principles and Applications*, VCH, New York, NY u.a 1994.
- [2] N. Berova, L. Di Bari, G. Pescitelli, *Chem. Soc. Rev.* **2007**, 36, 914.
- [3] W. Kuhn, *Trans. Faraday Soc.* **1930**, 26, 293.
- [4] C. L. Covington, P. L. Polavarapu, *J. Phys. Chem. A* **2013**, 117, 3377.
- [5] C. L. Covington, P. L. Polavarapu, *Phys. Chem. Chem. Phys.* **2016**, 18, 13912.
- [6] F. Santoro, F. Mortaheb, J. Lepelmeier, U. Boesl, U. Heiz, A. Kartouzian, *ChemPhysChem* **2018**, 19, 715.
- [7] F. Pulm, J. Schramm, J. Hormes, S. Grimme, S. D. Peyerimhoff, *Chem. Phys.* **1997**, 224, 143.
- [8] D. E. Bays, G. W. Cannon, R. C. Cookson, *J. Chem. Soc. B* **1966**, pages 885–892.
- [9] N. Lin, F. Santoro, X. Zhao, A. Rizzo, V. Barone, *J. Phys. Chem. A* **2008**, 112, 12401.
- [10] S. Feinleib, F. A. Bovey, *Chem. Commun. (London)* **1968**, pages 978–979.
- [11] U. Boesl, A. Bornschlegl, C. Logé, K. Titze, *Anal. Bioanal. Chem.* **2013**, 405, 6913.
- [12] C. Logé, A. Bornschlegl, U. Boesl, *Anal. Bioanal. Chem.* **2009**, 395, 1631.
- [13] R. Li, R. Sullivan, W. Al-Basheer, R. M. Pagni, R. N. Compton, *J. Chem. Phys.* **2006**, 125, 144304.
- [14] D. W. Urry, *Annu. Rev. Phys. Chem.* **1968**, 19, 477.
- [15] H. P. J. M. Dekkers, L. E. Closs, *J. Am. Chem. Soc.* **1976**, 98, 2210.
- [16] K. Titze, T. Zollitsch, U. Heiz, U. Boesl, *ChemPhysChem* **2014**, 15, 2762.
- [17] P. Horsch, G. Urbasch, K.-M. Weitzel, D. Kröner, *Phys. Chem. Chem. Phys.* **2011**, 13, 2378.
- [18] H. G. Breunig, G. Urbasch, P. Horsch, J. Cordes, U. Koert, K.-M. Weitzel, *ChemPhysChem* **2009**, 10, 1199.
- [19] U. Boesl von Grafenstein, A. Bornschlegl, *ChemPhysChem* **2006**, 7, 2085.
- [20] A. Bornschlegl, C. Logé, U. Boesl, *Chem. Phys. Lett.* **2007**, 447, 187.
- [21] T. Ring, C. Witte, S. Vasudevan, S. Das, S. T. Ranecky, H. Lee, N. Ladda, A. Senftleben, H. Braun, T. Baumert, *Rev. Sci. Instrum.* **2021**, 92, 033001.
- [22] W. Moffitt, A. Moscovitz, *J. Chem. Phys.* **1959**, 30, 648.
- [23] O. E. Weigang Jr., *J. Chem. Phys.* **1965**, 42, 2244.
- [24] J. Franck, E. G. Dymond, *Trans. Faraday Soc.* **1926**, 21, 536.
- [25] E. Condon, *Phys. Rev.* **1926**, 28, 1182.
- [26] E. U. Condon, *Phys. Rev.* **1928**, 32, 858.
- [27] G. Herzberg, E. Teller, *Z. Phys. Chem.* **1933**, 21B, 410.
- [28] M. Born, R. Oppenheimer, *Ann. Phys.* **1927**, 389, 457.
- [29] S. Bernadotte, A. J. Atkins, C. R. Jacob, *J. Chem. Phys.* **2012**, 137, 204106.
- [30] L. D. Barron, *Molecular light scattering and optical activity*, Cambridge University Press, Cambridge, UK, 2nd ed., rev. and enl edition **2004**.
- [31] P. W. Atkins, R. S. Friedman, *Molecular Quantum Mechanics*, Oxford University Press, Oxford, 3. edition **1997**.
- [32] J. A. Schellman, *Chem. Rev.* **1975**, 75, 323.
- [33] W. J. Meath, E. A. Power, *J. Phys. B: Atom. Mol. Phys.* **1987**, 20, 1945.
- [34] E. U. Condon, *Rev. Mod. Phys.* **1937**, 9, 432.
- [35] M. Pecul, K. Ruud, *Adv. Quantum Chem.* **2005**, 50, 185.
- [36] R. D. Gillard, P. R. Mitchell, *Trans. Faraday Soc.* **1969**, 65, 2611.
- [37] J. He, A. G. Petrovic, P. L. Polavarapu, *J. Phys. Chem. B* **2004**, 108, 20451.
- [38] W. Al-Basheer, R. M. Pagni, R. N. Compton, *J. Phys. Chem. A* **2007**, 111, 2293.
- [39] J. Huh, R. Berger, *J. Phys. Conf. Ser.* **2012**, 380, 012019.
- [40] D. J. Tannor, E. J. Heller, *J. Chem. Phys.* **1982**, 77, 202.
- [41] S. Abbate, G. Longhi, K. Kwon, A. Moscovitz, *J. Chem. Phys.* **1998**, 108, 50.
- [42] J. Seibt, V. Engel, *J. Chem. Phys.* **2007**, 126, 074110.
- [43] J. Huh, *Unified description of vibronic transitions with coherent states*, Ph.D. thesis, Johann Wolfgang Goethe-Universität, Frankfurt am Main **2011**.
- [44] R. Ahlrichs, M. Bär, M. Häser, H. Horn, C. Kölmel, *Chem. Phys. Lett.* **1989**, 162, 165.
- [45] F. Weigend, *Phys. Chem. Chem. Phys.* **2006**, 8, 1057.
- [46] F. Weigend, R. Ahlrichs, *Phys. Chem. Chem. Phys.* **2005**, 7, 3297.
- [47] A. D. Becke, *Phys. Rev. A* **1988**, 38, 3098.
- [48] C. Lee, W. Yang, R. G. Parr, *Phys. Rev. B* **1988**, 37, 785.
- [49] K. Eichkorn, O. Treutler, H. Öhm, M. Häser, R. Ahlrichs, *Chem. Phys. Lett.* **1995**, 240, 283.
- [50] S. Grimme, J. Antony, S. Ehrlich, H. Krieg, *J. Chem. Phys.* **2010**, 132, 154104.
- [51] S. Grimme, S. Ehrlich, L. Goerigk, *J. Comput. Chem.* **2011**, 32, 1456.
- [52] See Supporting Information for this article for further details on geometry optimizations and results of the quantum chemical calculations.
- [53] R. Berger, C. Fischer, M. Klessinger, *J. Phys. Chem. A* **1998**, 102, 7157.
- [54] H.-C. Jankowiak, J. L. Stuber, R. Berger, *J. Chem. Phys.* **2007**, 127, 234101.
- [55] S. Coriani, T. Kjærgaard, P. Jørgensen, K. Ruud, J. Huh, R. Berger, *J. Chem. Theory Comput.* **2010**, 6, 1028.
- [56] D. Kim, T. Baer, *Chem. Phys.* **2000**, 256, 251.
- [57] G. Orlandi, W. Siebrand, *J. Chem. Phys.* **1973**, 58, 4513.
- [58] L. Levin, W. Skomorowski, L. Rybak, R. Kosloff, C. P. Koch, Z. Amitay, *Phys. Rev. Lett.* **2015**, 114, 233003.
- [59] L. Levin, D. M. Reich, M. Geva, R. Kosloff, C. P. Koch, Z. Amitay, *J. Phys. B: At. Mol. Opt. Phys.* **2021**, 54, 144007.
- [60] M. Mondelo-Martell, D. Basilewitsch, H. Braun, C. P. Koch, D. M. Reich, *Phys. Chem. Chem. Phys.* **2022**, 24, 9286.

Manuscript received: September 18, 2024
 Revised manuscript received: December 9, 2024
 Accepted manuscript online: December 23, 2024
 Version of record online: ■■, ■■

RESEARCH ARTICLE

Anisotropy factor spectra for the weak $n \rightarrow \pi^*$ -type A-band of chiral ketones cannot be described within the Franck–Condon approximation. Thus, we present such spectra computed by accounting for Herzberg–Teller corrections and compare them to experiments for fenchone, camphor and 3MCP to describe chiroptical properties of these molecules in the mid to near ultraviolet.



L. A. Kerber, O. Kreuz, T. Ring, Dr. H. Braun, Prof. Dr. R. Berger, Dr. D. M. Reich*

1 – 10

Anisotropy Factor Spectra for Weakly Allowed Electronic Transitions in Chiral Ketones

